

Tectonic stress field and fractal distribution of volcanoes in the Michoacán-Guanajuato region of the Mexican Volcanic Belt

Ken Kurokawa¹, Kenshiro Otsuki¹ and Toshiaki Hasenaka²

¹ Department of Geoenvironmental Sciences, Faculty of Science, Tohoku University, Sendai, Japan.

² Institute of Mineralogy, Petrology and Economic Geology, Faculty of Science, Tohoku University, Japan.

Received: April 20, 1994; accepted: January 10, 1995.

RESUMEN

El campo de esfuerzos tectónicos del Campo Volcánico de Michoacán-Guanajuato es estimado a partir de la orientación de fallas normales y del alineamiento de los volcanes: σ_1 (el esfuerzo principal compresional máximo) es vertical en toda la región y σ_2 se orienta E-W en el área norte y NE-SW en el área sur. El origen del campo de esfuerzos es atribuido al deslizamiento en dirección a la trinchera de la porción de arco sobre la superficie del límite quebradizo/dúctil inducido por el enrollamiento del eje de la Trinchera Mesoamericana. Esto se atribuye a la tasa de subducción de la Placa de Cocos que es más lenta que la tasa crítica de 7.2 cm/año. La distribución espacial de los centros volcánicos y el volumen de los cuerpos volcánicos son fractales; las dimensiones fractales son 1.63 y 1.44 respectivamente. El origen de la fractalidad y los valores elevados de la dimensión fractal son explicados mediante una analogía con la interdigitación viscosa o invasión percolante en medio poroso que es un efecto del perfil del esfuerzo cortical del campo de esfuerzos tensional.

PALABRAS CLAVE: Tectónica, campo de esfuerzos, volcanes, fractales, Faja Volcánica Trans-Mexicana, Michoacán.

ABSTRACT

From the orientation of normal faults and the alignment of volcanoes, the tectonic stress field of the Michoacán-Guanajuato volcanic field was estimated. The maximum compressional principal stress σ_1 is vertical throughout the region and σ_2 trends E-W in the northern area and NE-SW in the southern area. The origin of the stress field is attributed to the trenchward slipping of the arc sliver on the brittle/ductile boundary surface induced by the rollback of the Middle America trench axis. This is related to the subduction rate of the Cocos plate which is slower than the critical rate of 7.2 cm/y. The spatial distribution of volcanic centers, and the volume of volcanic bodies, are fractal; the fractal dimensions are 1.63 and 1.44 respectively. The fractality and the large values of the fractal dimension are explained by an analogy to viscous fingering or invasion percolation in porous media which is an effect of the crustal stress profile of the tensional stress field.

KEY WORDS: Tectonics, stress field, volcanoes, fractals, Mexican Volcanic Belt, Michoacán.

INTRODUCTION AND GEOLOGIC BACKGROUND

The subduction of the Cocos plate at the Middle America trench and the subduction of the Rivera plate at the Acapulco trench are associated with active arc volcanism. The Mexican volcanic belt extends more than 1000 km in an east-west direction (Figure 1). The convergence rate between the Cocos and North America plates is 7 cm/y at the trench off eastern Mexico, decreasing westward to 5 cm/y off the Michoacán-Guanajuato volcanic field (MGVF). The gap between the Middle America trench and the volcanic front is about 400 km in the east and it decreases westward to 200 km, consistent with the changes in dip angle of the deep seismic zone (Burbach *et al.*, 1984) and the convergence rate between the Cocos and North America plates. The maximum depth of the seismic zone is more than 200 km in the region subducted by the Cocos plate (Burbach *et al.*, 1984). On the other hand, the convergence rate between the Rivera and North America plates is much slower, 2 cm/y in the south decreasing northward (DeMets and Stein, 1990). The position of the deep seismic zone is unclear and the hypocenters are shallower than 200 km (Eissler and McNally, 1984).

The central Mexican arc is now in an extensional tectonic regime. The graben system from west to east consists

of: Tepic-Zacoalco graben, Chapala graben, Cuitzeo graben and Acambay graben within the Mexican volcanic belt (Figure 2). The orientation of the intermediate principal stress (σ_2) is nearly parallel to the graben system but it diverges on the north and south (Pasquaré *et al.*, 1988a; Suter, 1991; Suter *et al.*, 1992). The main objective of our paper is to confirm the stress field of the MGVF and to propose a new idea for the origin of the stress field in agreement with plate kinematics.

The volcanoes in the Mexican volcanic belt, where a tensional stress field prevails, contrast strongly with those in the northeast Japan arc which is under a compressional stress field. The Mexican volcanoes are monogenetic and exhibit a closely spaced distribution, while the Japanese volcanoes are polygenetic and form widely separated clusters. The second objective of our paper is to explain these differences in volcanic style from the viewpoint of viscous fingering or invasion percolation affected by the stress field, by using the fractal distribution of volcanoes as a clue.

STRESS FIELD RECONSTRUCTION BY FAULT ANALYSIS

We researched neotectonic faults using 1/50,000 topographic map sheets published by DETENAL (Mexico) and

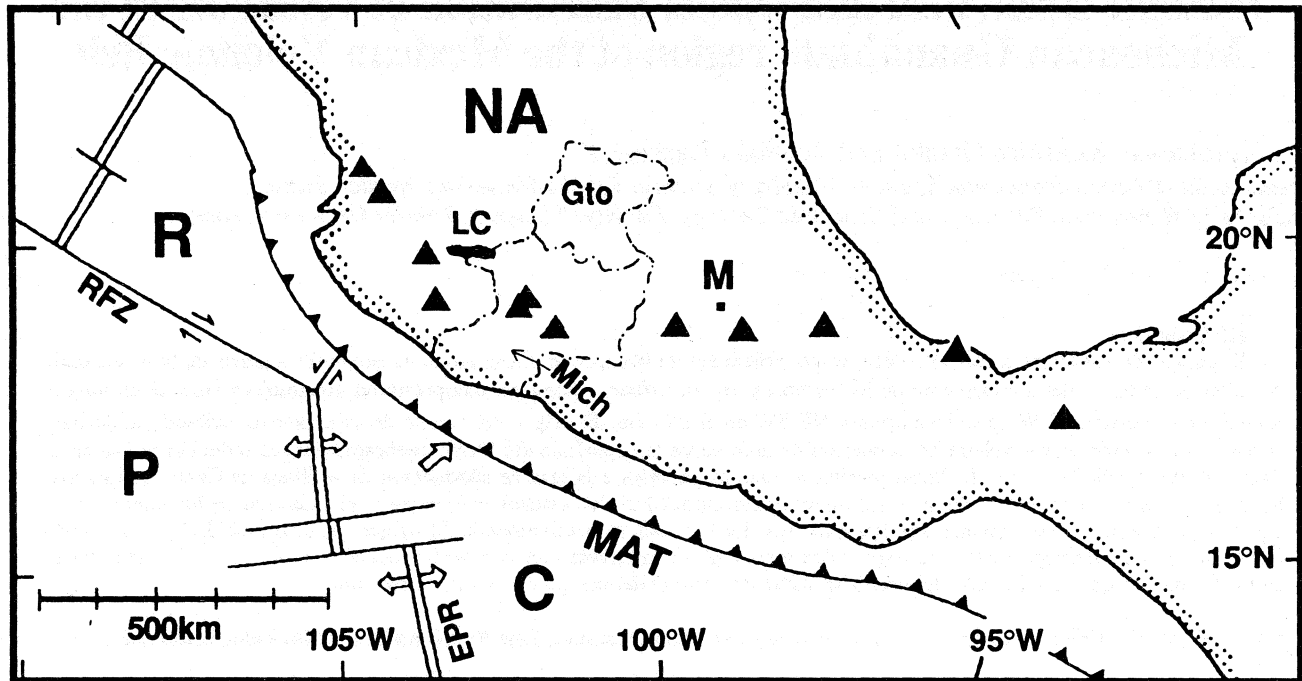


Fig. 1. Plate tectonic framework of the Mexican arc and its adjacent region. NA: North America plate, P: Pacific plate, C: Cocos plate, R: Rivera plate, EPR: East Pacific rise, RFZ: Rivera fracture zone, MAT: Middle America trench, M: Mexico City, LC: Lake Chapala, Mich: state of Michoacán, Gto: state of Guanajuato, solid triangle: active volcanoes.

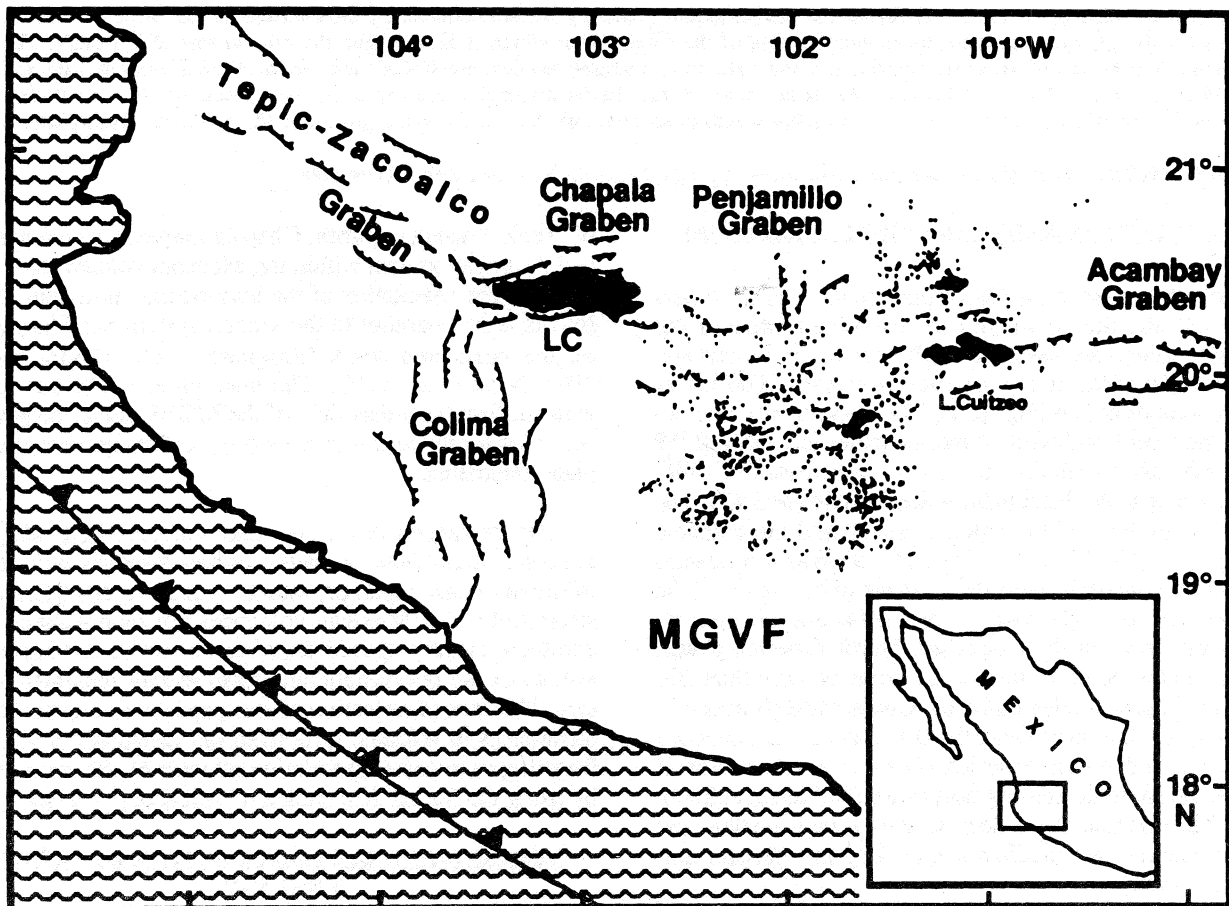


Fig. 2. Graben system in the western Mexican arc. Small dots denote volcanic cones in the Michoacán-Guanajuato volcanic field (MGVF) from Hasenaka and Carmichael (1985a).

air photographs within a quadrangle defined by 100°20'W~102°40'W, 19°N~20°45'N. Faults are well developed in the region to the north of 19°45'N (Figure 3), but rare in the south where volcanoes younger than 1 Ma are widely distributed. In the northwestern area, WNW-ESE trending faults are dominant, which are the eastern continuation of the Chapala rift system. In the northeastern area, ENE-WSW trending faults are well developed, partly forming the Cuitzeo graben. Few N-S trending faults are associated with the central part forming the Penjamillo graben. All of these are normal faults, and a maximum throw of 300 m may be read from the topographic contours. No lateral component of fault displacement is detected from the offset of river channels and mountain ridges; however, Pasquaré *et al.* (1988a) detected a small component of sinistral motion along E-W trending normal faults which were active in the Pleistocene time in the Cuitzeo Lake area.

Many shield volcanoes are offset by ENE-WSW, E-W or WNW-ESE trending normal faults. Cerro Brinco del Diablo (shown in Figure 4), a typical case, is cut by two ENE-WSW trending normal faults, and the zone between them including the volcanic center is dropped down. Along

these faults no lateral offset is found at streams and ridges. Similar structures are also found for many other volcanoes, for example Cerro Grande in the Moroleon map sheet and Cerro El Varal in the Puruandiro sheet.

As mentioned above, most of the faults in the study area are normal and the fault traces of the conjugate fault set are nearly parallel, suggesting that the axis of maximum compressional principal stress σ_1 is vertical and the other two axes of principal stresses are in the horizontal plane. The lateral change in direction of these fault traces suggests that the axes of intermediate stress σ_2 and minimum principal stress σ_3 trend WNW-ESE and NNE-SSW, respectively in the northwestern area, and ENE-WSW and NNW-SSE in the northeastern area. However, the significance of the N-S trending normal fault system forming the Penjamillo graben in the central area is unclear. Johnson and Harrison (1990) attributed its origin to the uplift due to shallow intrusion of a large magma body.

Some of the E-W trending normal faults (including WNW-ESE and ENE-WSW trending fault systems) have a north side throw and others have a south side throw. They

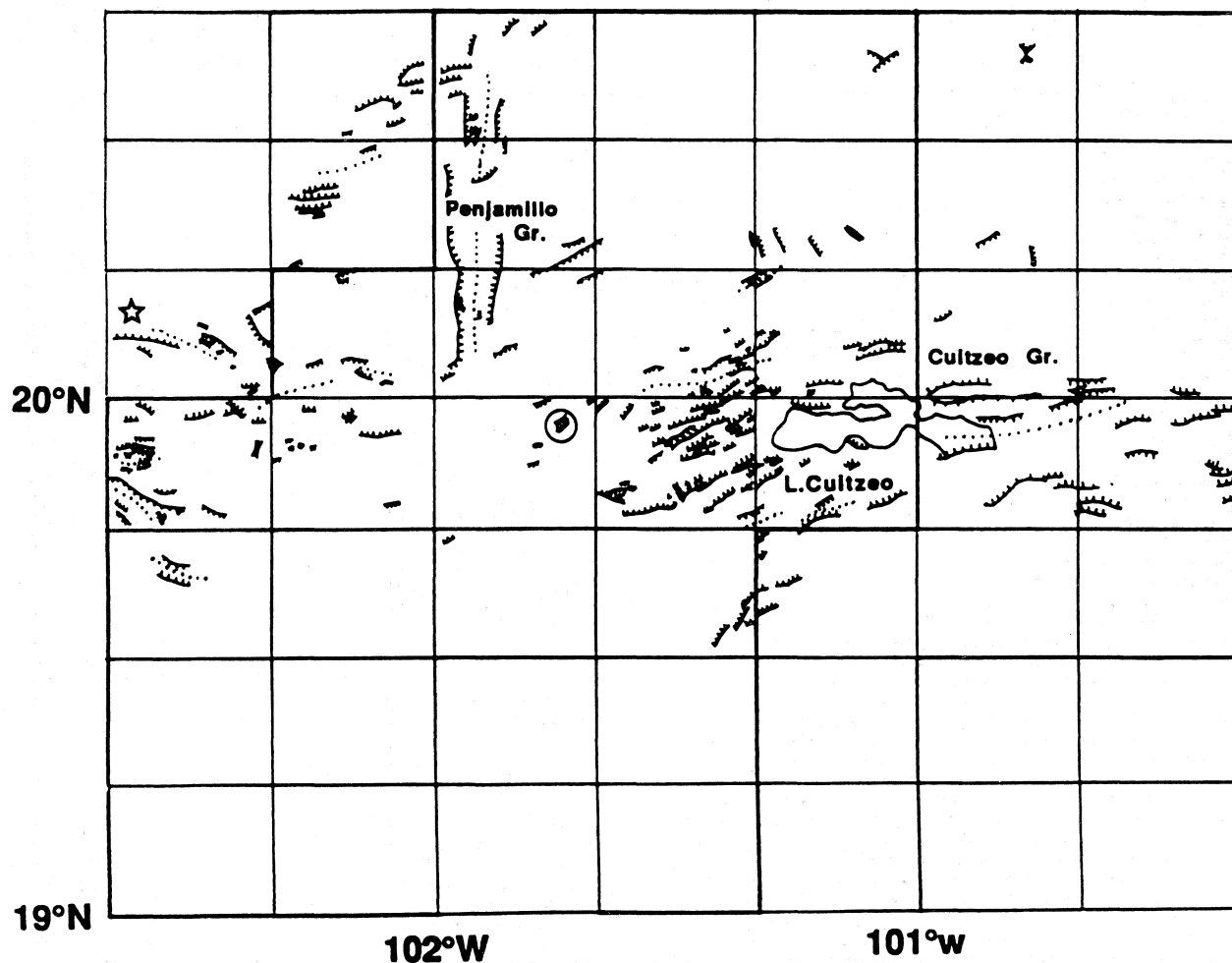


Fig. 3. Distribution of faults. The faults in the area on the east of the 101°W longitudinal line are after Suter *et al.* (1992). ○: locality of Cerro Brinco del Diablo. ☆: epicenter of the earthquake on the E-W trending fault at Pajacuaran (Delgado-Granados, personal communication).axis of symmetry of half grabens.

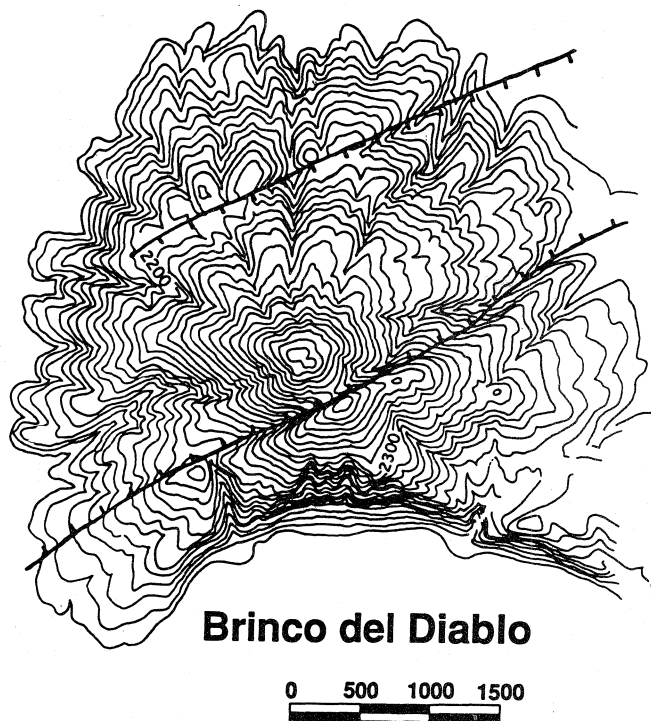


Fig. 4. Two normal faults cutting Cerro Brinco del Diablo.

appear to form a conjugate fault set, but locally one or the other is dominantly developed; thus the asymmetric development of conjugate normal faults and the axial line of symmetry can be drawn only locally (Figure 3). Nevertheless, the axial lines concentrate around the 20°N latitudinal line. It is known that the asymmetric development of normal faults is controlled by the horizontal gradient of extensional stress (or strain), and that faults with fault planes inclined toward the region of high tensional stress are selectively developed (Ishikawa and Otsuki, 1995). Hence the tensional stress is maximum along a 20°N latitudinal line. It is reasonable to assume that the line of maximum stress coincides with the zone of the maximum geothermal gradient, as the upper part of the crust of low temperature and hence with high strength is thinnest there. This is a reason why most of the grabens developed within the Mexican volcanic belt.

STRESS FIELD RECONSTRUCTION BY ALIGNMENT OF VOLCANOES

In the MGVF, which occupies an area of 40,000 km², 1040 small volcanoes (scoria cones, lava cones, tuff cones, maars, lava domes and thick lava flows) and 378 medium-size volcanoes (shield volcanoes, stratovolcanoes and large lava domes) may be counted (Figure 5, after Hasenaka and Carmichael, 1985a, 1985b and Hasenaka, 1994). The small volcanoes consist mainly of basalts and basaltic andesites, whereas the medium size ones are andesitic. They appear to be distributed at random but some cones form linear clusters (Hasenaka and Carmichael, 1985b; Pasquaré et al., 1988b). According to Nakamura (1977), flank volcanic centers are aligned with the "maximum" principal stress

within the horizontal plane, as fissure orientation is controlled by stress concentration around the center of magma conduit. The orientation of "maximum" principal stresses estimated by this method is the axis of σ_1 or σ_2 projected onto the horizontal plane. Here we write the "maximum" principal stress as σ_{Hmax} . The alignments of about 30 clusters of volcanic cones which are easily recognized without any data processing are plotted in Figure 6 (open bar). They show a regional tendency; NE-SW south of the 19°30'N latitudinal line and ENE-WSW north of it.

At a glance, the cones arranged linearly are only about 10% of the total. But the prevalence of alignment can be detected as follows. First, measure the position vector from one volcano (volcano 1 in Figure 7) to its nearest neighbor (volcano 2) and another vector from volcano 2 to its nearest neighbor (volcano 3) other than volcano 1. Now, measure the clockwise angle θ between the two position vectors. Repeat the procedure for all volcanoes and count the frequency of volcanoes in each 10 degrees interval of θ . Figure 8 shows the relation between θ and the probability converted from the frequency, for small cones and shield volcanoes. Both have a maximum probability at $\theta=0^\circ$, suggesting an alignment of volcanoes. The peak probability for cones is very sharp and stronger than for shield volcanoes which have a multimodal and broad peak. Hence cones are arranged more linearly than shield volcanoes and are more stress-sensitive than the latter.

Wadge and Cross (1988) and Connor (1990) tried to detect the alignment of volcanoes in the MGVF by statistical methods. Following Fly (1979), suppose an assemblage of n points in a Cartesian coordinate system (Figure 9). Draw position vectors from any point to the other $n-1$ points, and repeat the procedure for all points. Remove all position vectors without rotating and adjust their starting points to the origin. We now have an assemblage of $(n-1)n$ terminal points of the vectors. In this type of figure the original pattern, including the linear arrangement of spatial distribution of points, is exaggerated $n-1$ times.

We drew Fly maps of volcanic cones for every 1/50,000 topographic map sheet (some examples are shown in Figure 10). By looking at a Fly map from a low angle while rotating it, the linear arrangements may be visualized more clearly. Sharp and thin alignments are more significant than broad ones because the linear arrangements which we seek are those controlled by crustal fissures. In the Fly map for sheet A14, for example, the terminal points of the position vectors form an elliptical outline. The orientation of the long axis of the ellipse merely reflects the elliptic distribution of the cones within the map sheet; but the sharp and thin alignment at N78°E may be regarded as the appropriate orientation of σ_{Hmax} . For three other map sheets (A32, A41 and B39), lineaments with slightly different orientations may be recognized; in each case the solid lines are clearer than the broken lines. The orientations of the alignments detected by the Fly method for all topographic maps are plotted in Figure 6 (solid bar). The length of a bar denotes qualitatively the clearness of the alignment. The result adds new orientation data. For

MICHOACAN-GUANAJUATO VOLCANIC FIELD

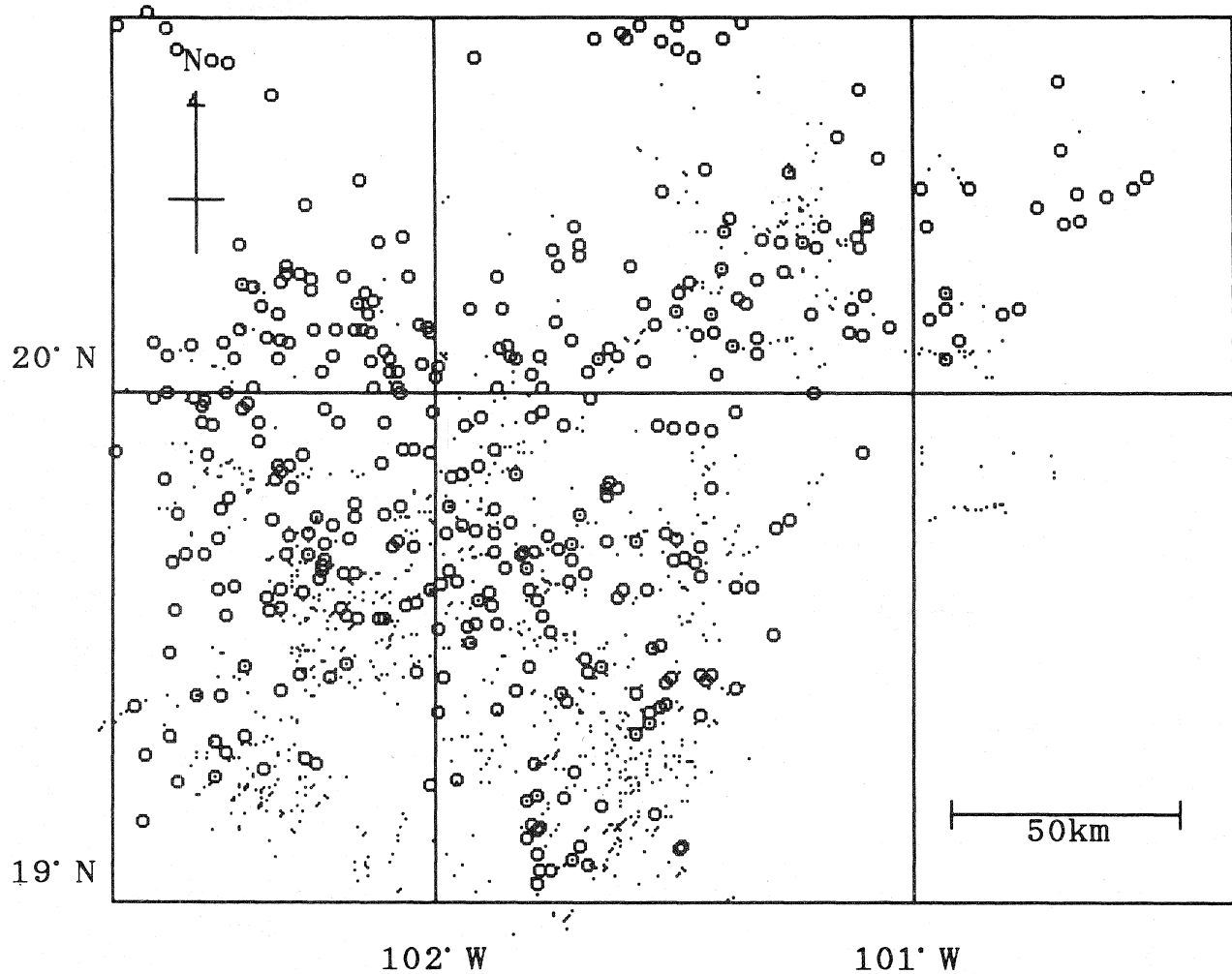


Fig. 5. Distribution of shield volcanoes (open circles) and volcanic cones (small dots) in the Michoacán-Guanajuato volcanic field, after Hasenaka and Carmichael (1985a).

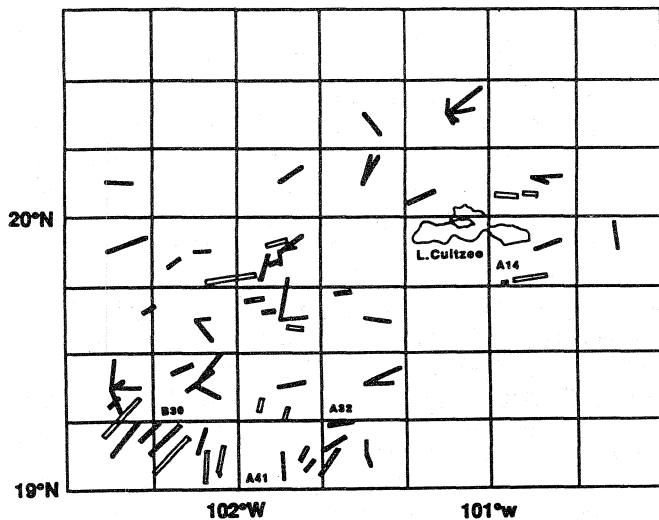


Fig. 6. Linearly arranged clusters of small volcanic cones (open bars), and the volcanic lineaments detected by the Fly method (solid bars) for each 1/50,000 map sheet studied.

some map sheets the solid bars are inconsistent with the open bars, but generally they agree.

We conclude that the orientation of σ_{Hmax} is ENE-WSW in the area north of latitude 19°30'N, i.e. nearly parallel to the trace of the normal faults; and that it changes to NE-SW south of that latitude.

TECTONIC IMPLICATIONS OF STRESS FIELD

According to Ban *et al.* (1992), the ages of the volcanoes south of about 20°N latitude are younger than 1 Ma (0~0.87 Ma) while those in the northern area are older (1.17~2.78 Ma). Hence the stress field estimated from the distribution of normal faults north of about 20°N latitude is younger than about 3 Ma. For example, Cerro Brinco del Diablo (Figure 4) whose age is 1.88 Ma (Ban *et al.*, 1992), is cut by normal faults. The stress field estimated from the aligned volcanoes south of about 20°N latitude is younger than 1 Ma. Between latitudes 19°30'N and 20°N the young volcanoes and normal faults are coeval, and the orientation of σ_2 estimated from faults and of σ_{Hmax} esti-

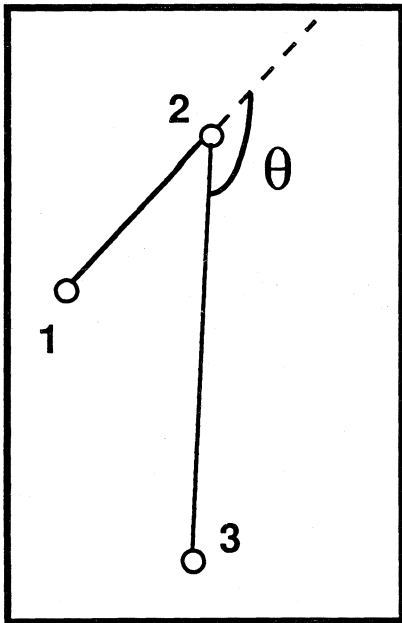


Fig. 7. Illustration of the procedure to quantify the linear arrangement of volcanoes. The details of the procedure are in the text.

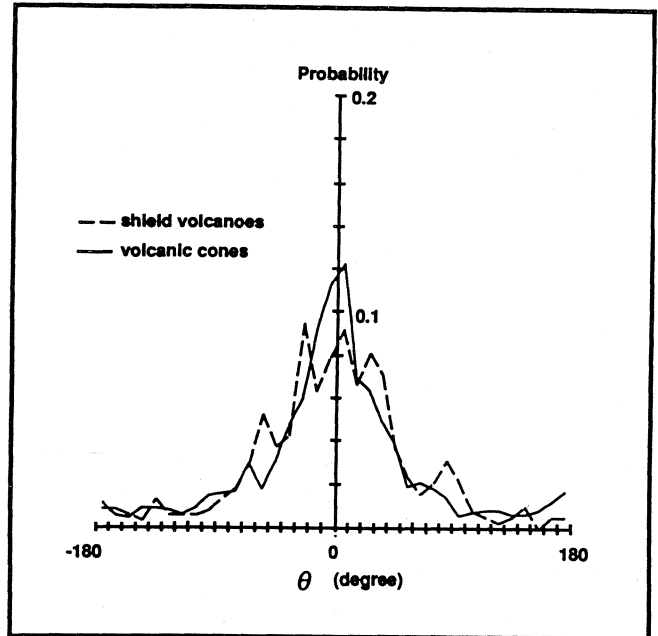


Fig. 8. The probability at which three volcanic cones (solid line) and three shield volcanoes (broken line) exist within each 10° interval of θ in Fig. 7.

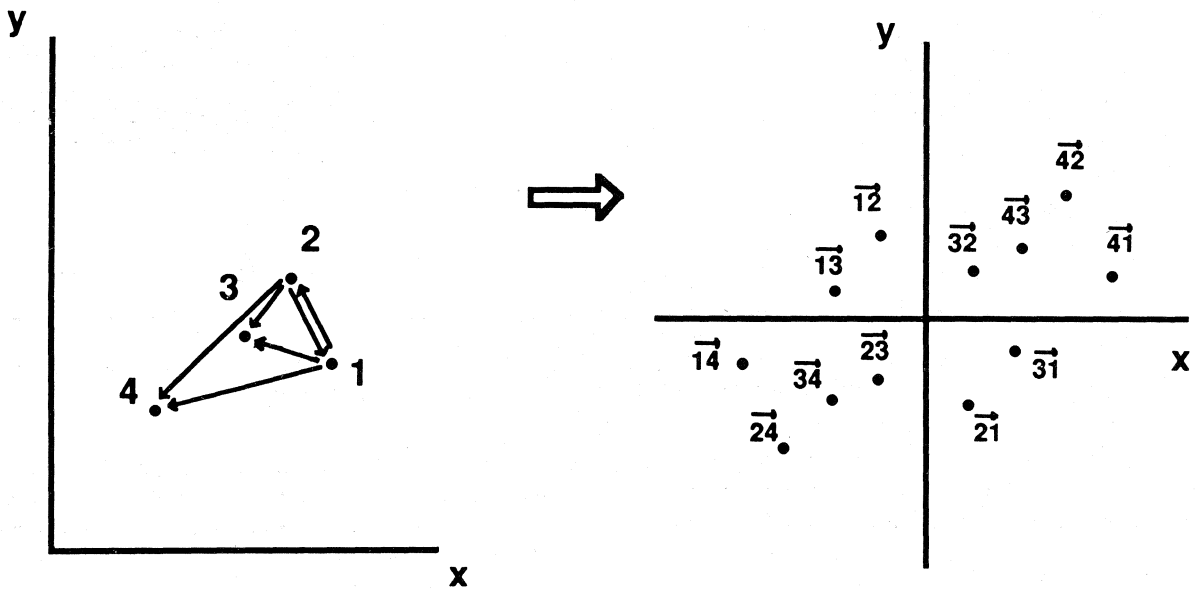


Fig. 9. Illustration of the procedure for constructing the Fly map. The details of the procedure are in the text.

mated from linearly arranged volcanoes are mutually consistent (see Figure 3 and Figure 6). This fact suggests; (1) that σ_{Hmax} corresponds to σ_2 , and (2) that the stress field estimated from faulting extended until after 1 Ma.

Cerro El Picacho ($19^\circ 50' 20'' N$, $101^\circ 58' 01'' W$) whose age is 0.17 Ma (Ban *et al.*, 1992) and the neighboring three stratovolcanoes are aligned in an ENE-WSW direction and their slope is cut by a normal fault of the same trend. Seis-

mic activity is known on the E-W trending fault at Pajacuaran (Delgado-Granados, personal communication) and on the E-W trending Venta de Bravo fault to the west of the Lake Cuitzeo (Suter *et al.*, 1992). Therefore, the stress field reconstructed from faults must be active until the present.

We conclude that the stress fields estimated by the two methods can be combined into a single figure which repre-

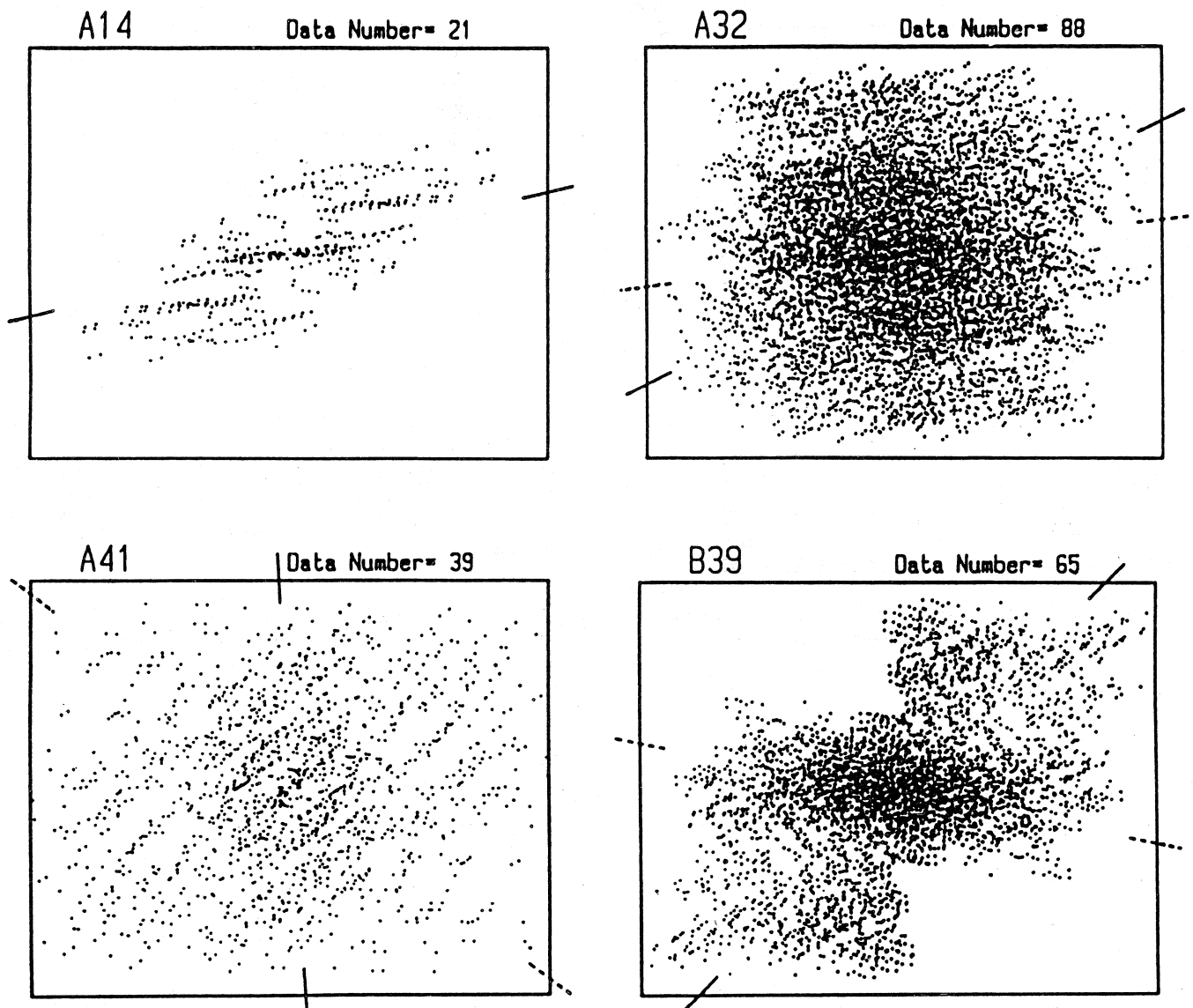


Fig. 10. Examples of Fly maps for volcanic cones in four different 1/50,000 map sheets in the Michoacán-Guanajuato volcanic field. Solid and broken marker lines denote the volcanic lineaments.

sents the stress field in the period from about 1 Ma to the present. It is characterized by a N-S trending σ_3 and an E-W trending σ_2 in the north (rear), and a NW-SE trending σ_3 and a NE-SW trending σ_2 in the south (front). The initiation of this stress field may be older than 1 Ma, but we have no data for the assignment of its oldest age. The fact that there are few faults in the southern area may suggest that the differential stress in the front is smaller in magnitude than in the rear. Suter (1991) compiled present-day stress orientation data over Mexico and western Central America. According to his results, σ_{Hmax} trends E-W (N-S tension) in the Mexican Volcanic Belt, N-S (E-W tension) to the north and NE-SW (NW-SE tension) to the south. The stress field that we propose is consistent with this result.

One problem is the origin of the N-S trending tensional stress in the Mexican volcanic belt. Suter (1991) at-

tributed it to bending due to volcanic and topographic loads. We propose to solve this problem by plate kinematics. Extensional tectonics in the Mexican arc is consistent with the first law of convergence rate of plates by Otsuki (1989). This rule states that the extension rate of arc crust is equal to 7.2 cm/y minus the convergence rate when the seismic zone is deeper than 200 km, or to 3.4 cm/y minus the rate of plate convergence when it is shallower than 200 km. The convergence rate between the Cocos and North America plates is 5 to 6 cm/y (NUVEL-1; DeMets *et al.*, 1990), decreasing northwestward along the Middle America trench. Hence we can expect 1 to 2 cm/y of crustal extension for the central and eastern part of the Mexican arc. For the western part of the Mexican arc under which the Rivera plate is subducting, the convergence rate is 1.5~2 cm/y (DeMets and Stein, 1990) and the deep seismic zone is shallower than 200 km, thus a 1 to 2 cm/y crustal extension rate is also expected. In conclusion, we can expect a

crustal extension rate of 1~2 cm/y over the Mexican arc. Extensional deformation is concentrated in the zone of high geothermal gradients where strong crust is thinned, resulting in a zone of prominent graben systems along the axis of the Mexican Volcanic Belt.

The next problem is to explain why σ_2 trends NE-SW in the frontal side and why the horizontal differential stress is small there. DeMets and Stein (1990) proposed that the southeastward translation of the arc sliver (the Michoacán and Guerrero blocks) at several mm/y is due to the oblique subduction of the Cocos plate. Their idea is supported by data for sinistral slip on the Chapala-Oaxaca and Chapala-Tula fault zones (Johnson and Harrison, 1990), and E-W trending normal faults in the central sector of the Mexican Volcanic Belt (Pasquaré et al., 1988a; Suter et al., 1992). It is possible for the orientation of σ_2 to be distorted to NE-SW on the frontal side by sinistral shear in the arc sliver due to oblique subduction. In order to explain why the horizontal differential stress in the frontal side is smaller than that in the rear side, we may modify the suggestion by DeMets and Stein. According to the 2nd law of convergence rate of plates (Otsuki, 1989), the rollback rate of the trench axis is equal to the velocity of subducting plate minus 7.2 cm/y. Combining this with the 1st law, we conclude that extension at the Mexican arc is caused by the absolute rollback rate of the Middle America trench axis which is 1~2 cm/y faster than the southwestward absolute motion of the North American plate.

Consider that the force balance for an arc sliver is the resultant of the gravity force, the force on the subducting plate boundary, the force on the mechanical bottom surface of the arc sliver and the force on the vertical plane below the volcanic front (Figure 11). The mechanical bottom surface of the arc sliver is assumed to be at the brittle/ductile boundary, which dips trenchward because the geothermal gradient in general decreases trenchward. Following the laws of convergence rate of plates, the surface force on the vertical plane below the volcanic front is zero when the convergence rate is 7.2 cm/y, and the horizontal components of the other three forces balance. When the convergence rate is less than 7.2 cm/y, in the Mexican arc, the decrease of the compressional force on the subducting plate boundary due to the oceanward motion of the trench axis causes a trenchward slip of the arc sliver along the brittle/ductile boundary, producing a graben system in the zone of arc volcanism. The new force balance in this case is achieved among forces including the frictional force on the brittle/ductile boundary and the tensional force on the vertical plane below the graben system. This new force balance brings about a gradient of horizontal stress in the arc sliver increasing trenchward, which explains the smaller horizontal differential stress at the frontal side of the Mexican arc than at the rear.

FRACTAL DISTRIBUTION OF VOLCANOES

The density of volcanic centers is very high in the Michoacán-Guanajuato Volcanic Field (MGVF) in comparison with other island-arc volcanic belts. It is true that the

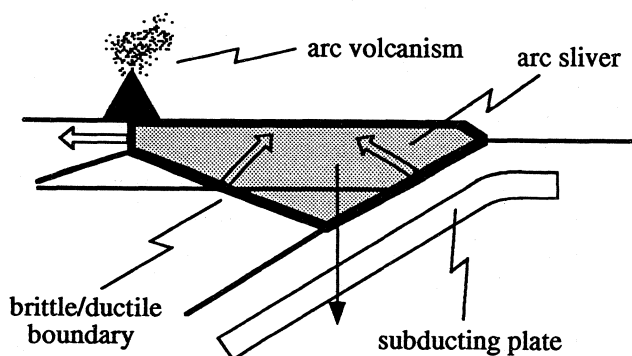


Fig. 11. Force balance for arc sliver. The details are in the text.

density changes from area to area in the volcanic region. However, it appears that high and low-density areas are themselves composed of subareas of high and low density (Figure 5). This is a fractal distribution. Let us test the fractality by using the fractal dimension (e.g., Feder, 1988) as defined below.

At first, the volcanic field is divided into a mesh of $L \times L$ km. If $P_i(L)$ is defined as the probability of occurrence of volcanic centers in the i -th mesh, the total information $I(L)$ is given by;

$$I(L) = -\sum P_i(L) \log P_i(L)$$

When L is variable, and the relation between L and $I(L)$ is written as

$$I(L) = A - D \log L,$$

D is called information fractal dimension.

Figure 12a shows the relation between L and $I(L)$ for shield volcanoes, small cones and for all volcanic centers combined. This suggests a fractal distribution with $D \cong 1.63$ which is almost the same for the three cases. If a volcanic body with volume V is regarded as an assemblage of V volcanoes of unit volume, the fractal dimension for the spatial distribution of volumes of volcanoes can be calculated by the same method. Figure 12b shows the spatial distribution of volumes of volcanoes using the data by Hasenaka and Carmichael (1985a), yielding a fractal dimension of $D \cong 1.44$. The fractality for the distribution of the centers of volcanic cones plus shield volcanoes holds best, even in the range of small L . On the other hand, the fractality for volcanic volumes breaks down in the range $L < 15$ km when the volumes of shield volcanoes are counted. These facts suggest that the distribution of magma conduits underground is fractal as a whole, and that additional factors control the volume distribution of magma ascending through the conduits.

In order to discover the factors which cause the volume distribution to deviate from a fractal relation in the range $L < 15$, we measured the distance from a volcano to its near-

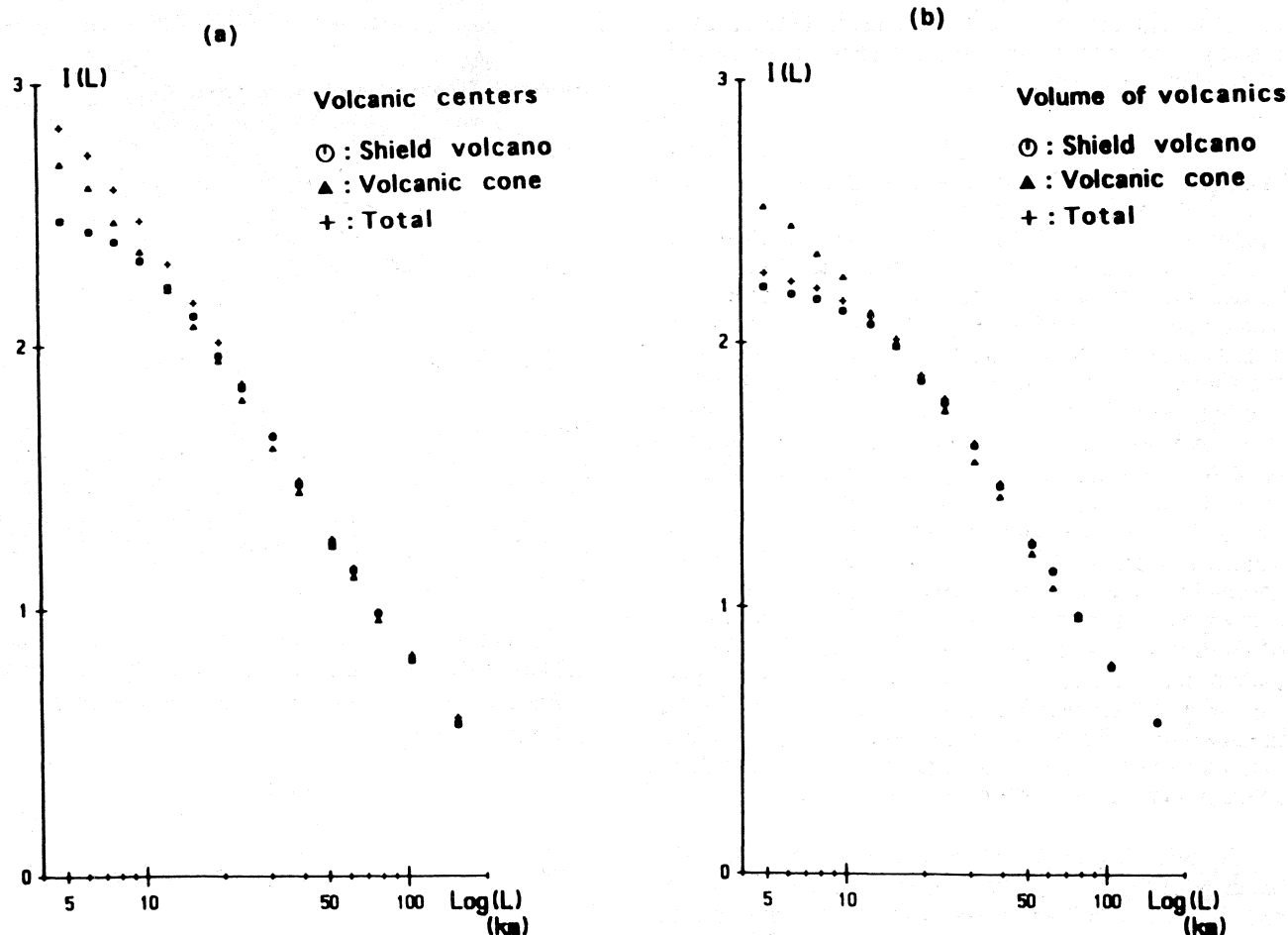


Fig. 12. Relationships between the scales of observation L and the total information $I(L)$ for position of volcanic centers (a) and for volume of volcanic bodies (b).

est neighbor and we calculated the probability at which the nearest volcano is found within 250 m intervals for small cones and within 1 km intervals for shield volcanoes (Figure 13). The probability is maximum at about 1 km distance for volcanic cones and about 3 km for shield volcanoes. This suggests that the volcanoes of these two types have a proximal territory from which other volcanoes are excluded. The fact that the territory size of shield volcanoes is larger than that of cones suggests that the territorialism is related with the formation of magma conduits rather than with the process of magma transport.

TECTONIC SIGNIFICANCE OF FRACTAL DISTRIBUTION OF VOLCANOES

Magma transport in porous media (fractured earth crust) at a depth h is driven by the excess of magmatic pressure $p_m(h)$ over the normal stress $\sigma_n(h)$ at the surface of fractures. If the density of magma ρ_m is assumed to be constant and independent from h and the magma conduit is plugged at the surface, $p_m = \rho_m g h + \Delta p_{m0}$, where g is gravity and Δp_{m0} is the magmatic pressure at $h=0$. In contrast,

σ_n is a function of lithostatic pressure p_r and horizontal tectonic stress σ_t . Let θ be the dip angle of the fracture plane, then $\sigma_n = p_r + \sigma_t \sin^2 \theta$. If we assume that the rock density is constant and independent of h and if it is nearly equal to that of magma, then $p_r \approx \rho_m g h$. Tectonic stress σ_t can be estimated roughly from the flow-law of crustal rocks and the frictional sliding criteria as a function of h (e.g. Ord and Hobbs, 1989).

In the above context, $p_r(h)$, $p_m(h)$ and $\sigma_n(h)$ are drawn schematically in Figure 14. When σ_t is positive (compressional), $\sigma_n > p_r$, and vice versa. Note that the line of $p_m(h)$ crosses the line of $\sigma_n(h)$ when σ_t is compressional and Δp_{m0} is smaller than $\sigma_t \sin^2 \theta$ at the depth of the brittle/ductile boundary. In this case magma is prevented from rising and forms magma reservoirs just below the brittle/ductile boundary. When the condition $\Delta p_{m0} > \sigma_t \sin^2 \theta$ is satisfied at this depth by the increase of Δp_{m0} due to heating of the magma reservoir or by other causes, magmatic explosions will occur. In contrast, when σ_t is negative (tensional), the condition $\Delta p_{m0} > \sigma_t \sin^2 \theta$ is satisfied at all depths. No magma reservoir will form and the

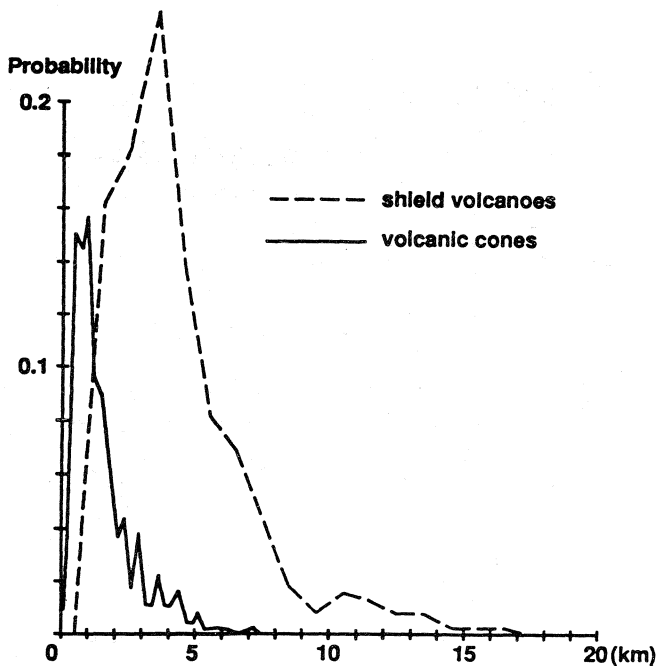


Fig. 13. The probability at which a nearest neighbor volcanic center occurs within each 250 m interval for volcanic cones (solid line) and within each 1 km interval for shield volcanoes (broken line).

magma will rise and flow out without a violent explosion. This explanation may be applied to the case of the MGVF. Over 200 chemical analyses of volcanic samples from the MGVF show that they are less fractionated (rich in MgO and poor in SiO₂) than lavas from large composite volcanoes in Mexico and elsewhere (Hasenaka and Carmichael, 1987). Several samples including those of Jorullo volcano (Luhr and Carmichael, 1985) show a primitive character that indicates equilibrium with mantle peridotites. Thus most MGVF magmas probably reached the surface without stagnation.

Another important parameter for the mode of magma transport is $\partial(p_m - \sigma_n) / \partial h$ ($\equiv \Delta\sigma$). When $\Delta\sigma > 0$, magma ascent is decelerated, and it is accelerated when $\Delta\sigma < 0$. This physical condition resembles viscous fingering or invasion percolation in porous media, both of which lead to a fractal distribution of the surface boundary of the injecting liquid. In the case where σ_t is compressional, $\Delta\sigma > 0$ below the brittle/ductile boundary and $\Delta\sigma < 0$ above it; hence bifurcation of the magma conduit in a fractal manner occurs only above the brittle ductile boundary. The brittle/ductile boundary is very shallow (several km) in regions of high thermal gradient such as arc magmatic belts; hence the depth interval is not sufficient for the magma conduit to bifurcate widely. Such a configuration of the magma conduit, in conjunction with the existence of a magma reservoir, results in polygenetic volcanoes forming widely-spaced clusters (Figure 15a) as in the northeast Japan arc. In contrast, the conditions are $\Delta\sigma < 0$ below the brittle/ductile boundary and $\Delta\sigma > 0$ above it when σ_t is ten-

sional. Then the magma conduit will bifurcate widely below the boundary, which is the major part of the traveling path for magma transport. Such a configuration of the magma conduit, in conjunction with no magma reservoir, causes a closely-spaced distribution of monogenetic and small volcanoes (Figure 15b) as in the MGVF.

Whether the tectonic stress is tensional or compressional, the distribution of volcanic centers is expected to be fractal. The fractal dimension is higher in the tensional case than in the compressional case. This appears to be supported by the tendency for volcanoes in arcs of compressional type, e. g. the Andes or northeast Japan, to be polygenetic and to distribute sporadically. In arcs of tensional type, like the Mexican Volcanic Belt and the Izu-Bonin arc, on the other hand, we find closely-spaced monogenetic volcanoes. In the backarc spreading stage, arc volcanism around the volcanic front is much weaker than in other types of arcs, and the magma supply is concentrated in the backarc spreading center, producing oceanic crust with an area proportional to the time lapse. The dimension of the distribution of the oceanic crust is 2, not

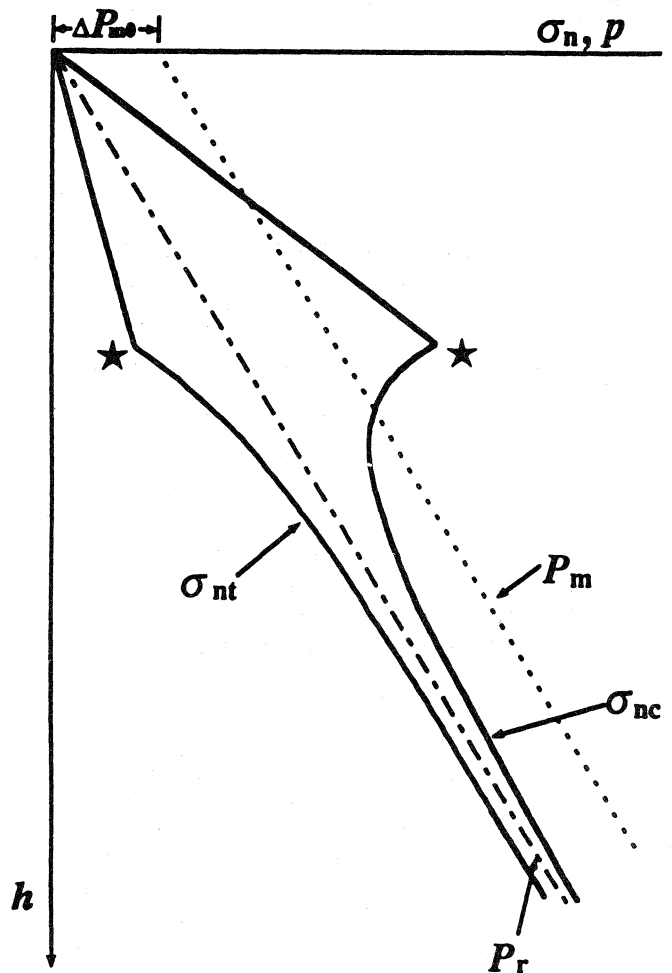


Fig. 14. Qualitative stress profile depending on the subsurface depth h . p_r : lithostatic pressure. p_m : magmatic pressure. σ_{nc} and σ_{nt} : normal stress on the fracture plane when horizontal tectonic stress is compressional and tensional, respectively. \star : depth of brittle/ductile boundary.

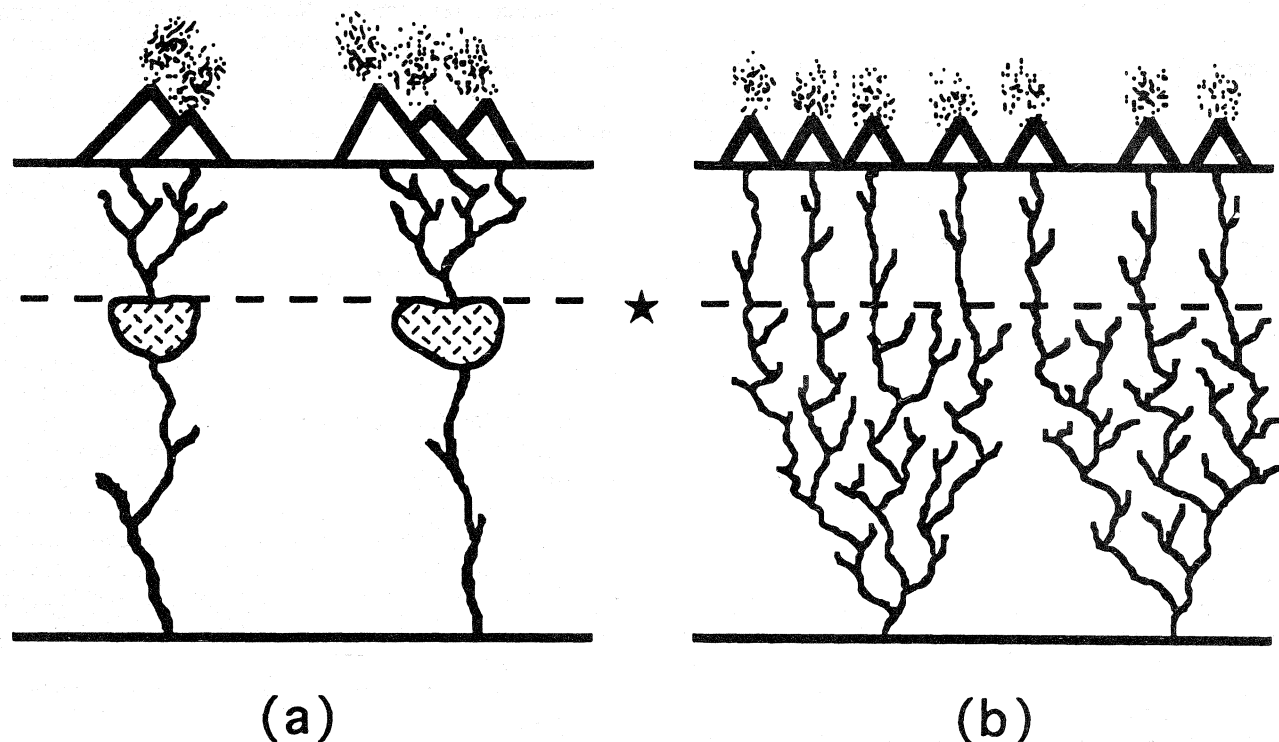


Fig. 15. Schematic illustrations showing the pattern of magma conduits and the type of volcanoes when horizontal tectonic stress is compressional (a) and tensional (b). ★: depth of brittle/ductile boundary. The shaded parts just below the brittle/ductile boundary in the left figure denote magma reservoirs.

fractal. Summarizing the relationship between the fractal dimension of the spatial distribution of volcanoes and the state of tectonic stress, we conclude that the fractal dimension may be small under compressional stress and increases with tectonic tensional stress until it attains a value of 2 when the backarc is spreading.

CONCLUSIONS

(1) The tectonic stress field of the Michoacán-Guanajuato volcanic field is divided into two domains: N-S trending σ_3 and E-W trending σ_2 in the rear, north of $19^{\circ}10'N$ latitude, and NW-SE trending σ_3 and NE-SW trending σ_2 in the front. The horizontal differential stress is high in the former and low in the latter.

(2) The origin of these stress fields is explained by (a) the convergence rate between the Cocos and North America plates which is 1~2 cm/y slower than the critical value of 7.2 cm/y, (b) the rollback rate of the western Middle America trench axis which is 1~2 cm/y faster than the oceanward motion of the North America plate, and (c) the force balance for the arc sliver and the oblique subduction of the Cocos plate.

(3) The spatial distribution of volcanoes in the Michoacán-Guanajuato region has two characteristics. The volcanic centers and the volumes of volcanic bodies show a fractal distribution when the scales of observation are larger than some critical scale. The most probable volcano spac-

ing is found; it is 1 km for volcanic cones and 3 km for shield volcanoes.

(4) These two characteristics suggest that the distribution of magma conduits and the process of magma transport are controlled by viscous fingering or invasion percolation in porous media and the territorialism of volcanoes.

(5) A qualitative consideration on the effect of crustal stress profile on viscous fingering or invasion percolation leads us to the conclusion that a volcanic field characterized by closely spaced monogenetic volcanoes with a high fractal dimension, such as the Michoacán-Guanajuato region, is related to a tensional stress regime.

ACKNOWLEDGMENTS

Part of our scientific results was obtained from a 1991 joint project between Tohoku University and UNAM, Mexico (Monbuso International Scientific Research Program No.03041014). Thanks are due to Prof. emeritus K. Aoki who organized the project, and to all members of the project. We are much indebted to Dr. H. Delgado-Granados for fruitful discussions and generous guidance of our field survey.

BIBLIOGRAPHY

BAN, M., T. HASENAKA, H. DELGADO-GRANADOS and N. TAKAOKA, 1992. K-Ar ages of lavas from

- shield volcanoes in the Michoacán-Guanajuato volcanic field, Mexico. *Geofís. Int.*, 31, 467-473.
- BURBACH, G.V., C. FROHLICH, W.D. PENNINGTON and T. MATSUMOTO, 1984. Seismicity and tectonics of the subducted Cocos plate. *J. Geophys. Res.*, 89, 7719-7735.
- CONNOR, C. B., 1990. Cinder cone clustering in the Trans-Mexican Volcanic Belt: implications for structural and petrologic models. *J. Geophys. Res.*, 95, 19,396-19405.
- DeMETS, C., R. G. GORDON, D. F. ARGUS and S. STEIN, 1990. Current plate motions. *Geophys. J. Int.*, 101, 425-478.
- DeMETS, C. and S. STEIN, 1990. Present-day kinematics of the Rivera plate and implications for tectonics in southwestern Mexico. *J. Geophys. Res.*, 95, 21931-21948.
- EISSLER, H. K. and K. C. McNALLY, 1984. Seismicity and tectonics of the Rivera plate and implications for the 1932 Jalisco, Mexico, earthquake. *J. Geophys. Res.*, 89, 4520-4530.
- FEDER, J., 1988. *Fractals*, Plenum Press, New York., 283 pp.
- FLY, N., 1979. Random point distribution and strain measurement in rocks. *Tectonophysics*, 60, 89-105.
- HASENAKA, T., 1994. Size, distribution, and magma output rate for shield volcanoes of the Michoacán-Guanajuato volcanic field, Mexico. *J. Volcanol. Geotherm. Res.*, 63, 13-31.
- HASENAKA, T. and I. S. E. CARMICHAEL, 1985a. A compilation of location, size, and geomorphological parameters of volcanoes of the Michoacán-Guanajuato volcanic field, central Mexico. *Geofís. Int.*, 24, 577-607.
- HASENAKA, T. and I.S.E. CARMICHAEL, 1985b. The cinder cones of Michoacán-Guanajuato, central Mexico: their age, volume and magma discharge rate. *J. Volcanol. Geotherm. Res.*, 25, 105-124.
- HASENAKA, T. and I. S. E. CARMICHAEL, 1987. The cinder cones of Michoacán-Guanajuato, central Mexico: petrology and chemistry. *J. Petrol.*, 28, 241-269.
- ISHIKAWA, M. and K. OTSUKI, 1995. The effects of strain gradients on the asymmetry of experimental normal fault system. *J. Struct. Geol.*, in press.
- JOHNSON, C.A. and C.G.A. HARRISON, 1990. Neotectonics in central Mexico. *Phys. Earth Planet. Interiors*, 64, 187-210.
- LUHR, J. F. and I. S. E. CARMICHAEL, 1985. Jorullo volcano, Michoacán, Mexico (1759-1774): the earliest stages of fractionation in calc-alkaline magmas. *Contrib. Mineral. Petrol.*, 90, 142-161.
- NAKAMURA, K., 1977. Volcanoes as possible indicators of tectonic stress orientation. Principle and proposal. *J. Volcanol. Geoth. Res.*, 2, 1-16.
- ORD, A. and B.E. HOBBS, 1989. The strength of the continental crust, detachment zones and the development of plastic instabilities. *Tectonophysics*, 158, 269-289.
- OTSUKI, K., 1989. Empirical relationships among the convergence rate of plate, rollback rate of trench axis and island-arc tectonics: "laws of convergence rate of plates". *Tectonophysics*, 159, 73-94.
- PASQUARÈ, G., V.H. GARDUÑO, A. TIBALDI and M. FERRARI, 1988a. Stress pattern evolution in the central sector of the Mexican volcanic belt. *Tectonophysics*, 146, 353-364.
- PASQUARÈ, G., A. TIBALDI, M. ATTOLINI and G. CECCONI, 1988b. Morphometry, spatial distribution and tectonic control of Quaternary volcanoes in Northern Michoacán, Mexico. *Rendiconti Della Società Italiana di Mineralogia e Petrologia.*, 43, 1215-1225.
- SUTER, M., 1991. State of stress and active deformation in Mexico and western Central America. In: *The Geology of North America Decade Map, Volume 1*, 401-421.
- SUTER, M., O. QUINTERO and C.A. JOHNSON, 1992. Active faults and state of stress in the central part of the Trans-Mexican volcanic belt, Mexico. 1. The Venta de Bravo fault. *J. Geophys. Res.*, 97, 11983-11993.
- WADGE, G. and A. CROSS, 1988. Quantitative methods for detecting aligned points: An application to the volcanic vents of the Michoacán-Guanajuato volcanic field, Mexico. *Geology*, 16, 815-818.

Ken Kurokawa¹, Kenshiro Otsuki¹ and Toshiaki Hasenaka²

¹ Department of Geoenvironmental Sciences, Faculty of Science, Tohoku University, Aobayama, Sendai, 980-77 Japan.

² Institute of Mineralogy, Petrology and Economic Geology, Faculty of Science, Tohoku University, Aobayama, Sendai, 980-77 Japan.